Transport Model for Microfluidic Device for Cell Culture and Tissue Development

Mater. Res. Soc. Symp. Proc. Vol. 1299 © 2011 Materials Research Society
DOI: 10.1557/opl.2011.467

Transport Model for Microfluidic Device for Cell Culture and Tissue Development

Niraj Inamdar[1,2], Linda Griffith[2,3], Jeffrey T. Borenstein[1]

[1]Charles Stark Draper Laboratory, Inc., Department of Biomedical Engineering,
555 Technology Square, Cambridge, MA 02139, U.S.A.
[2]Massachusetts Institute of Technology, Department of Mechanical Engineering,
77 Massachusetts Avenue, Cambridge, MA 02139, U.S.A
[3]Massachusetts Institute of Technology, Department of Biological Engineering,
77 Massachusetts Avenue, Cambridge, MA 02139, U.S.A

ABSTRACT

In recent years, microfluidic devices have emerged as a platform in which to culture tissue for various applications such as drug discovery, toxicity testing, and fundamental investigations of cell-cell interactions. We examine the transport phenomena associated with gradients of soluble factors and oxygen in a microfluidic device for co-culture. This work focuses on emulating conditions known to be important in sustaining a viable culture of cells. Critical parameters include the flow and the resulting shear stresses, the transport of various soluble factors throughout the flow media, and the mechanical arrangement of the cells in the device. Using analytical models derived from first principles, we investigate interactions between flow conditions and transport in a microfluidic device. A particular device of interest is a bilayer configuration in which critical solutes such as oxygen are delivered through the media into one channel, transported across a nanoporous membrane, and consumed by cells cultured in another. The ability to control the flow conditions in this membrane bilayer device to achieve sufficient oxygenation without shear damage is shown to be superior to the case present in a single channel system. Using the results of these analyses, a set of criteria that characterize the geometric and transport properties of a robust microfluidic device are provided.

INTRODUCTION

Microfluidic devices have become a common platform on which biomedical diagnostics can be carried out and cell culture systems observed and engineered [1,2]. More specifically, these microfluidic devices have been applied towards organ transplant and organ assist [3], drug delivery[4], drug discovery [5], and bioassay [6] applications. A common configuration consists of a single microfluidic channel through which culture medium is flowed, with cells cultured on the bottom [7] (Figures 1a, 1c). In general, solute is introduced into the channel, with medium flowed directly over cells, and cellular behavior in response to solute concentration is observed.

As a consequence of fluid being flowed over the cell population, fluidic shear is imparted directly on the cells. However, it is known that cells' metabolic activity is sensitive to shear stresses [8,9,10]. It is very possible, then, that cellular responses that are measured are altered by the presence of shear. Moreover, delivering the same amount of solute to all the cells cultured may become a challenge, for in a single channel configuration, equitable delivery may only occur by increasing the flow rate and consequently, shear. Hence, it is also preferable experimentally to deliver a controlled quantity of solute to the cell population while at the same time having independent control over the imparted shear. We may attempt, then, to seek an alternative device configuration, some of which are analyzed in the literature, and utilize unique biologically-inspired [9] or grooved geometries [10] to shield cells from shear. Here, we will analyze the bilayer construct [1,11,12], which affords itself to a much more straightforward analysis and offers greater simplicity in the way of fabrication.

A bilayer device comprises two channels through which fluid may be flowed, and which are separated by a membrane (Figures 1b,1d). One channel may be used to populate the cell culture (the "cell compartment"), while the other may be used to flow medium containing the solute (the "flow channel"). Solute diffuses across the membrane and into the cell compartment where it is consumed by the cell population. The primary benefit of this construct is that the cells are not subjected to the shear forces of the flow channel, so we may vary that flow rate independently of the cell compartment's to deliver solute to cell compartment. We then only need to maintain a nominal perfusion flow in the cell compartment, while we may modulate the flow channel flow rate arbitrarily.

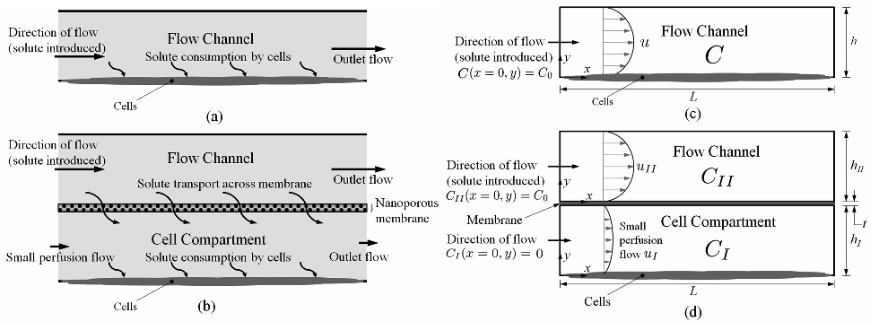

Figure 1. Schematic of (a) single channel and (b) bilayer configurations and geometry of (c) single channel and (d) bilayer configuration

THEORY

In order to establish the fundamental behavior of the configuration, we consider a simple, two-dimensional model with low Reynolds number flow with geometrical values as defined in Figures 1c and 1d. The equations governing transport in the channels are

$$u_i(y)\frac{\partial C_i}{\partial x} = D_i \frac{\partial^2 C_i}{\partial y^2}, \; i = I, II \tag{1}$$

where $u_i(y)$ is the velocity of the medium in the channel, given by

$$u_i(y) = \frac{h_i}{2\mu_i}\left(-\frac{\partial p_i}{\partial x}\right)\frac{y_i}{h_i}\left(1 - \frac{y_i}{h_i}\right), \; i = I, II \tag{2}$$

The shear imparted on the channel walls is given by

$$\tau_i = \mu_i \left.\frac{\partial u_i}{\partial y}\right|_{y=0,h_i} \tag{3}$$

where μ_i is the viscosity of the medium, and the boundary conditions in the flow channel are

(4)
$$\begin{cases} C_{II}(x=0,y)=C_0 \\ D_{II}\left.\dfrac{\partial C_{II}}{\partial y}\right|_{y=h_{II}}=0 \\ D_{II}\left.\dfrac{\partial C_{II}}{\partial y}\right|_{y=0}=\dfrac{D_{membrane}}{t}\left[C_{II}(x,y=0)-C_I(x,y=h_I)\right] \end{cases}$$

with prescribed inlet concentration, no-flux condition at the upper wall, and diffusion across the membrane. Boundary conditions in the cell compartment are

(5)
$$\begin{cases} C_I(x=0,y)=0 \\ D_I\left.\dfrac{\partial C_I}{\partial y}\right|_{y=h_I}=D_{II}\left.\dfrac{\partial C_{II}}{\partial y}\right|_{y=0} \\ D_I\left.\dfrac{\partial C_I}{\partial y}\right|_{y=0}=V_{max}\rho_{cells}\dfrac{C_I(x,y=0)}{K_M+C_I(x,y=0)} \\ \qquad\approx\dfrac{V_{max}\rho_{cells}}{K_M}C_I(x,y=0) \end{cases}$$

assuming no solute at inlet, and cells consuming solute according to first order approximation of Michaelis-Menten kinetics. In order to solve the system given by (1), (3) and (4), a separation of variables technique may be used by writing $C_i=\xi_i(x)\eta_i(y)$ and solving the resulting ordinary differential equations. The differential equation for $\eta_i(y)$ may be solved for by expressing it as a power series in y. Subsequently, the complete solution may be written as

(6)
$$C_{II}=C_0\sum_{i=1}^{\infty}A_{II,i}\exp\left(-\frac{\lambda_{II,i}^2 D_{II}}{4u_{0,II}}\frac{x}{h_I^2}\right)\eta_{II,i}(y/h_{II})$$

(7)
$$C_I=C_0\sum_{i=1}^{\infty}A_{I,i}\exp\left(-\frac{\lambda_{I,i}^2 D_I}{4u_{0,I}}\frac{x}{h_I^2}\right)\eta_{I,i}(y/h_I)$$

where $\lambda_{j,i}$ $(j=I,II)$ are the zeros of a characteristic polynomial determined by the boundary conditions (4) and (5) and each $\eta_{j,i}$ is characteristic to $\lambda_{j,i}$. The $A_{j,i}$ are determined from an orthogonality condition similar to that used in Fourier analysis, but extended for the case of two adjacent domains. Finally, solute consumption is given by

(8)
$$\text{Consumption}=D_I\left.\frac{\partial C_I}{\partial y}\right|_{y=0}=\frac{V_{max}\rho_{cells}}{K_M}C_I(x,y=0)$$

Plots of equations (7) and (8) for the bilayer and the equivalent for the single channel case were generated in MATLAB (see below).

RESULTS AND DISCUSSION

The model system is a hepatocyte culture consuming oxygen. Studies suggest metabolic activity is negatively affected when shear exceeds $\tau_{max}\equiv 1.4\,dynes/cm^2$ [8]; the flow rate Q_{max} associated with τ_{max} is $.72\,\mu L/min$. The hepatocytes are assumed to encounter a hypoxic environment *in vivo*, and the membrane diffusivity chosen is that for a typical polymeric membrane (*e.g.* polycarbonate or Nafion); all other parameters used are summarized in Table 1. For the bilayer, the concentration field and consumption in the cell compartment may be modulated by increasing the flow rate in the flow channel (Figures 2 and 3), while flow in the cell compartment may be kept at some nominal level. We can impose a more uniform concentration and consumption profile in the cell compartment without increasing Q_I and thus the shear imparted on the cells τ (Figures 2a, 2b, 2c, and 3). Overall transport may be increased by changing the membrane diffusivity, possible, for instance, if the membrane is composed of a crosslinked network (Figure 4).

Parameter	**Value**	**Note**
D_{II}, D_I	$3\times10^{-5} cm^2/s$	Diffusion coefficient for oxygen in water
$D_{membrane}$	$5\times10^{-6} cm^2/s$	Diffusion coefficient for oxygen in membrane
t	$10\mu m$	Thickness of membrane
μ	$1\times10^{-2}\ dyne\cdot s/cm^2$	Viscosity of water
h_I	$50\mu m$	Height of channel
w	$200\mu m$	Width of channel
L	$1.5cm$	Length of channel
V_{max}	$.5\times10^{-9} mol/s/10^6 cells$	Maximum uptake rate of oxygen
K_M	$.5mmHg = 8.5\times10^{-9}\ mol/cm^3$	Michaelis-Menten parameter for oxygen
C_{sat}	$2.15\times10^{-7} mol/cm^3$	Oxygen concentration at saturation
C_0	$2.15\times10^{-9} mol/cm^3$	$.01\times C_{sat}$, 1% saturation
ρ_{cells}	$2.5\times10^4 cells/cm^2$	Cell density
Q_{max}	$.72\mu L/min$	Flow rate; determined from maximum shear condition

Table 1: Summary of parameters used.

For comparison, the single channel profile was also calculated. Even if $Q = Q_{max}$, the concentration profile is highly nonuniform (Figures 2d and 3). Consumption downstream in the single channel case can only match that of the bilayer if flow rates and shear are increased several fold their maximum values (e.g. Figure 3, in which Q is increased to $7Q_{max}$ and τ to $7\tau_{max} = 9.8\, dynes/cm^2$).

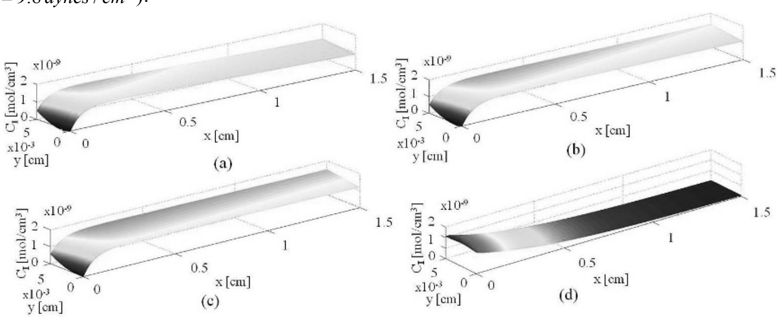

Figure 2. Surface plots of concentration fields as a function of space. For (a), (b) and (c), flow channel rates Q_{II} are $4.5\ \mu L/min$, $9.0\ \mu L/min$, and $18.0\ \mu L/min$, respectively, with cell compartment flow rate $Q_I = Q_{max}/2 = .36\mu L/min$. For (d), the single channel case, $Q = Q_{max} = .72\mu L/min$.

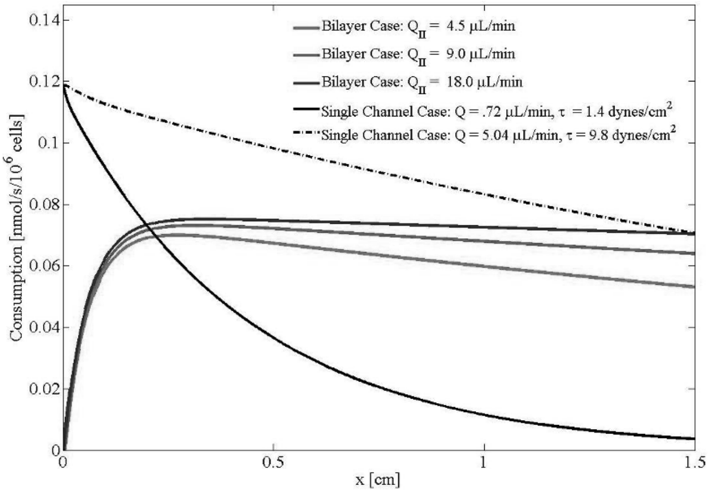

Figure 3: Comparison of bilayer and single channel consumption profiles. For bilayer case, $Q_I = Q_{max}/2 = .36\mu L/min$ (colored lines) with Q_{II} varied. $\tau = .7\ dynes/cm^2$ for each case. For the single channel case, $Q = Q_{max} = .72\mu L/min$ (solid black line) and $Q = 7Q_{max}$ (dotted black line).

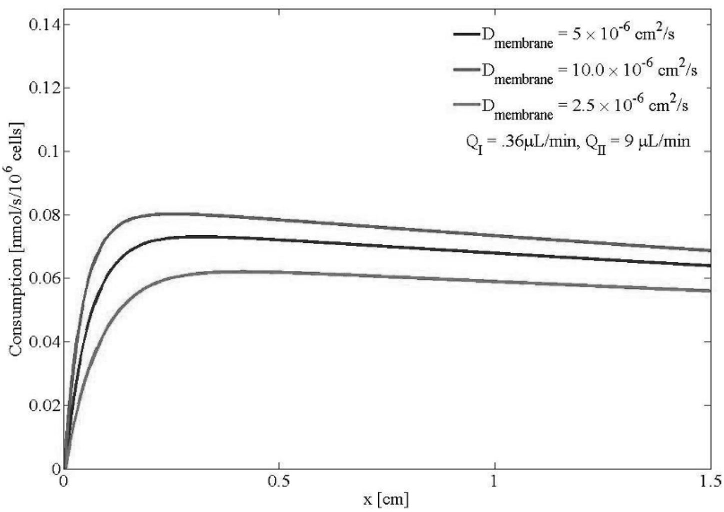

Figure 4. Increase in overall transport due to changes in membrane diffusivity. $D_{membrane}$ is $2.5\times10^{-6} cm^2/s$, $5.0\times10^{-6} cm^2/s$, and $7.5\times10^{-6} cm^2/s$.

CONCLUSIONS

We have considered and developed a solution to the problem of determining the concentration profile in a bilayer device. The bilayer offers a nearly uniform concentration profile, in direct contrast to the nonuniform profile of a standard single-channel device. The bilayer allows this profile to be delivered at a minimal level of shear, while in the single-channel device, transport cannot be made more uniform without increasing shear. It appears that this device configuration can offer a robust platform for future cell-culture experimentation, with modularity and control of solute delivery and microfluidic shear an intrinsic part of its operational capabilities. Validation and extension of the current model using numerical techniques is currently taking place with positive results, and experimental implementation of a cell-cultured bilayer device is under development.

ACKNOWLEDGMENTS

We gratefully acknowledge the support of the NIH NIBIB, grant # 5R01EB010246-02.

REFERENCES

1. A. Carraro, W. Hsu, K.M. Kulig, W.S. Cheung, M.L. Miller, E.J. Weinberg, E.F. Swart, M. Kaazempur-Mofrad, J.T. Borenstein, J.P. Vacanti, and C. Neville, Biomed. Microdevices, **10**, 795–805 (2008).
2. J.T. Borenstein, in *Comprehensive Microsystems*, edited by Y.B. Gianchandani, O. Tabata, and H. Zappe, (Elsevier , Amsterdam, 2005) **2**, pp. 541-584.
3. M.R. Kaazempur-Mofrad, J.P. Vacanti, N.J. Krebs, and J.T. Borenstein, Solid-State Sensor, Actuator and Microsystems Workshop, Hilton Head Island (2004).
4. Z. Chen, S.G. Kujawa, M.J. McKenna, J.O. Fiering, M.J. Mescher, J.T. Borenstein, E.E. Leary Swan, and W.F. Sewell*, J. Controlled Release*, **110**, 1-19 (2005).
5. D.A. LaVan, D.M. Lynn, and R. Langer, *Nature Reviews Drug Discovery*, **1**, 77-84 (2002).
6. S.K. Sia and G.M. Whitesides, *Electrophoresis*, **24**, 3563-3576 (2003).
7. Y. Zeng, T.S. Lee, P. Yu, P. Roy, and H.T. Low, *J. Biomech. Eng.*, **128**, 185-194 (2006)
8. Y. Tanaka, M. Yamato, T. Okano, T. Kitamori, and K. Sato, Meas. Sci. Technol., **17**, 3167-3170 (2006).
9. P.J. Lee, P.J. Hung, and L.P. Lee, *Biotechnol. Bioeng.*, 97, 1340-1346 (2007).
10. J. Park, F. Berthiaume, M. Toner, M. L. Yarmush, A. W. Tilles, *Biotechnol. Bioeng.*, **90**, 632-644 (2005).
11. D.M. Hoganson, J.L. Anderson, E.F. Weinberg, E.J. Swart, B.K. Orrick, J.T. Borenstein, and J.P. Vacanti, *J. Thorac. Cardiovasc. Surg.*, **140**, 990-995 (2010).
12. J.T. Borenstein, *Mater. Res. Soc. Symp. Proc.*, **1139**, 1139-GG02-01 (2008).